AD-A140 294 OBSERVATION OF RAYLEIGH-TAYLOR-LIKE STRUCTURES IN A LASER-ACCELERATED FOIL(U) NAVAL RESEARCH LAB WASHINGTON DC R R WHITLOCK ET AL. 19 MAR 84 NRL-MR-5204 1/1

UNCLASSIFIED F/G 17/8 NL

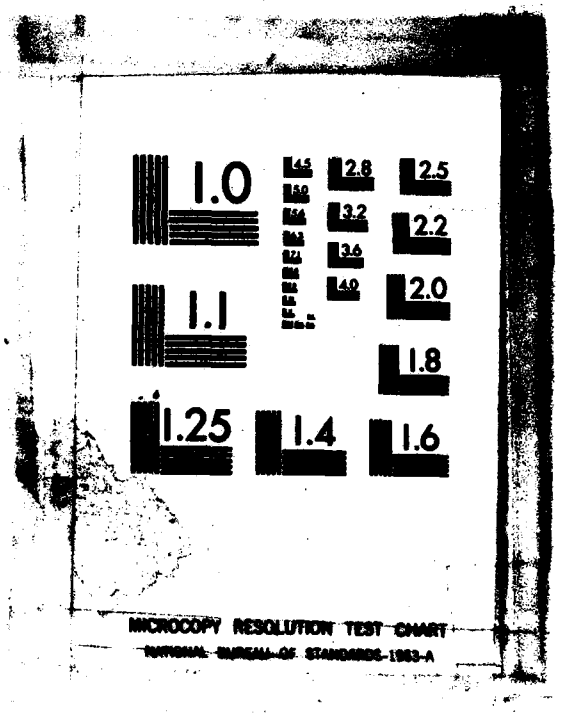
1.0
1.1
1.25
1.4
1.6
1.8
2.0
2.2
2.5
2.8
3.2
3.6
4.0
4.5
5.0
MICROCOPY RESOLUTION TEST CHART
NATIONAL BUREAU OF STANDARDS-1963-A

SECURITY CLASSIFICATION OF THIS PAGE

REPORT DOCUMENTATION PAGE

1a. REPORT SECURITY CLASSIFICATION Unclassified	1b. RESTRICTIVE MARKINGS
2a. SECURITY CLASSIFICATION AUTHORITY	3. DISTRIBUTION/AVAILABILITY OF REPORT Approved for public release; distribution unlimited.
2b. DECLASSIFICATION/DOWNGRADING SCHEDULE	
4. PERFORMING ORGANIZATION REPORT NUMBER(S) NRL Memorandum Report 5204	5. MONITORING ORGANIZATION REPORT NUMBER(S)
6a. NAME OF PERFORMING ORGANIZATION Naval Research Laboratory 6b. OFFICE SYMBOL (If applicable)	7a. NAME OF MONITORING ORGANIZATION
6c. ADDRESS (City, State and ZIP Code) Washington, DC 20375	7b. ADDRESS (City, State and ZIP Code)
8a. NAME OF FUNDING/SPONSORING ORGANIZATION Department of Energy 8b. OFFICE SYMBOL (If applicable)	9. PROCUREMENT INSTRUMENT IDENTIFICATION NUMBER
8c. ADDRESS (City, State and ZIP Code) 1000 Independence Avenue, S.W. Washington, DC 20545	10. SOURCE OF FUNDING NOS. PROGRAM ELEMENT NO. / PROJECT NO. / TASK NO. / WORK UNIT NO. 66-0859
11. TITLE (Include Security Classification) (See Page ii)	
12. PERSONAL AUTHOR(S) R. R. Whitlock, M. H. Emery, J. A. Stamper, E. A. McLean, S. P. Obenschain, and M. C. Peckerar	
13a. TYPE OF REPORT Interim 13b. TIME COVERED FROM _____ TO _____	14. DATE OF REPORT (Yr., Mo., Day) March 19, 1984 15. PAGE COUNT 9
16. SUPPLEMENTARY NOTATION	
17. COSATI CODES FIELD / GROUP / SUB. GR.	18. SUBJECT TERMS (Continue on reverse if necessary and identify by block number) Laser-produced plasma, Rayleigh-Taylor, flash x-ray backlighting, flash x radiography, hydrodynamic instability, inertial confinement fusion, spike, bubble, vortex, mass redistribution

19. ABSTRACT (Continue on reverse if necessary and identify by block number)

Laser-accelerated targets have been predicted to be subject to the Rayleigh-Taylor hydrodynamic instability. The development of the instability was studied by introducing mass thickness variations in foil targets and observing the development of the target nonuniformities by side-on flash x radiography. Observations were made of target structures and mass redistribution effects which resemble Rayleigh-Taylor bubbles and spikes, including not only advanced broadening of the spike tips on the laser-irradiated side of the foil but also projections of mass on the unirradiated side. The observations compare well with numerical simulations.

20. DISTRIBUTION/AVAILABILITY OF ABSTRACT UNCLASSIFIED/UNLIMITED ☒ SAME AS RPT. ☐ DTIC USERS ☐	21. ABSTRACT SECURITY CLASSIFICATION Unclassified
22a. NAME OF RESPONSIBLE INDIVIDUAL R. R. Whitlock	22b. TELEPHONE NUMBER (Include Area Code) (202) 767-2154 22c. OFFICE SYMBOL

DD FORM 1473, 83 APR EDITION OF 1 JAN 73 IS OBSOLETE.

SECURITY CLASSIFICATION OF THIS PAGE

11. TITLE (Include Security Classification)

OBSERVATION OF RAYLEIGH-TAYLOR-LIKE STRUCTURES IN A LASER-ACCELERATED FOIL

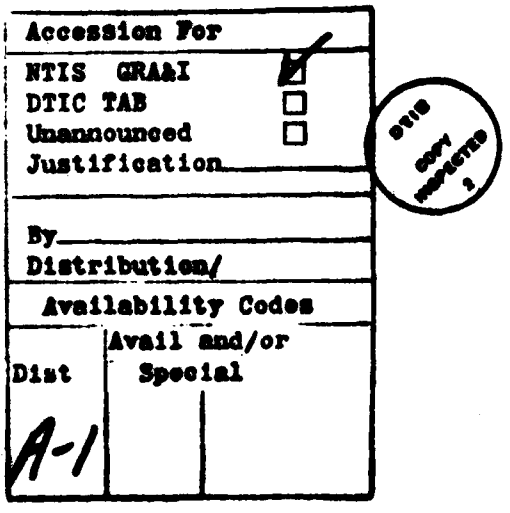

OBSERVATION OF RAYLEIGH-TAYLOR-LIKE STRUCTURES IN A LASER-ACCELERATED FOIL

The Rayleigh-Taylor[1] (RT) hydrodynamic instability can arise when a fluid of lower density accelerates a fluid layer of a higher density. The RT instability causes ripples at the interface between the fluids to grow in amplitude until the fluids interpenetrate each other as bubbles (of the lower density fluid) and spikes (of the higher density fluid), which can eventually shred the interface. The spikes grow as dense protrusions into the lighter material, locally increasing the mass thickness normal to the original interface. In the nonlinear regime, the spike-tips can develop a mushroom shape similar to a Kelvin-Helmholtz[2] rollup.[3] In addition, the confluence of mass into the spike can result in protrusions on the rear of the denser layer.[4] Using x radiography, we have obtained the first images of a laser-accelerated foil showing structures which resemble these Rayleigh-Taylor signatures. Such phenomena are of concern to inertial confinement fusion,[3-5] since implosion symmetry and fuel integrity may be spoiled by the RT instability.

Previous experiments with laser-accelerated targets without intentional target nonuniformities yielded no observable RT growth.[6] The first use of rippled and bar targets showed growth of initial perturbations, although the mechanisms remained in question.[7] Measured growth rates of mass modulations developing in corrugated foils, examined by streaked x radiography viewing normal to the foil, were in agreement with RT numerical simulations.[8] A face-on flash x-radiographic technique[9] using bar targets has recently shown evidence for RT growth.

In this work, planar foils were also structured periodically in mass thickness, in order to initiate the hydrodynamic instabilities with a predetermined wavelength. The spatial wavelength λ and thickness of the mass modulations were varied. The targets were made of plastic (1.0 g/cm^3), having rectangular bars of length L, of width $\lambda/2$ and separated by $\lambda/2$, placed on the rear (nonirradiated) side of a base foil. See Fig. 1. The foils were irradiated at 5×10^{12} W/cm^2 (computed from the temporal FWHM and the 90% energy contour of an equivalent focus) in the quasi-near field of a single driver beam of the Pharos II Nd: glass laser operating at 1.05 μm wavelength in a 4 ns pulse. The focal diameter was 650 μm. The bar length L for backlighting was 400 μm, i.e., less than the focal diameter. The laser's second beam was shortened to $\sim$300 ps and directed onto an adjacent Al target at 45° incidence to produce a flash backlighting source of 1.6 keV x rays[10] delayed $\sim$6 ns after the peak of the driver pulse. A pinhole array imaged the x-ray source and also viewed parallel to the bars on the foil to produce x radiographs at a magnification of 3.0; resolution was 10 μm, i.e., measurements are $\sim \pm 5$ μm. Another pinhole camera, behind and 20° from the target normal, recorded the self-emission of the accelerated foil and verified alignment of the bars.

Pyrometric blackbody brightness measurements[11] of the rear of the targets gave temperatures of only 4.5 $\pm$ 1. eV, regardless of target structure (unperturbed or λ = 8, 25, or 50 μm) on nonbacklighting shots, as well as on two backlighting shots. Thus, the backlighter did not appreciably heat the driven foil. Rear pinhole images and laser focal diagnostics showed circular fringes in the incident beam and also a pattern of 40-50 μm bands parallel to the bars in perturbed targets. The effects of this laser nonuniformity are observable in the original x radiograph of an accelerated unperturbed target as a gentle modulation in the accelerated target (Fig. 2b).

Manuscript approved January 27, 1984.

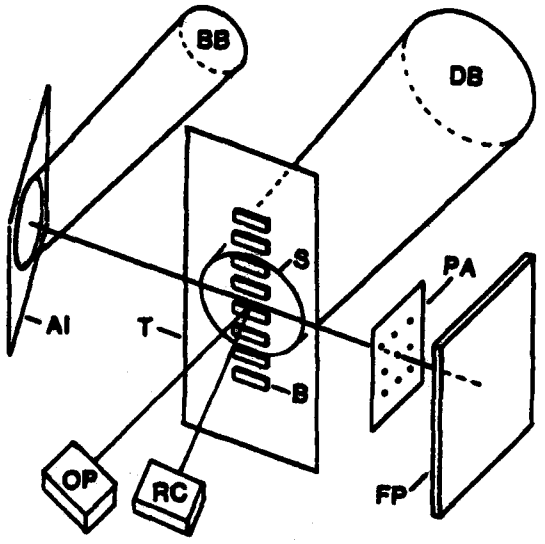

Fig. 1 — Setup. Driver laser beam (DB) was focused into a large spot (S) at 6° incidence onto a plastic foil target (T) having bars (B) on the rear. An optical pyrometer (OP) and a rear x-ray pinhole camera (RC) viewed from the rear. A second laser beam (BB) irradiated an Al target (Al) to provide a backlighting x-ray flash for radiography of the accelerated foil using a pinhole array (PA) to image onto a film pack (FP).

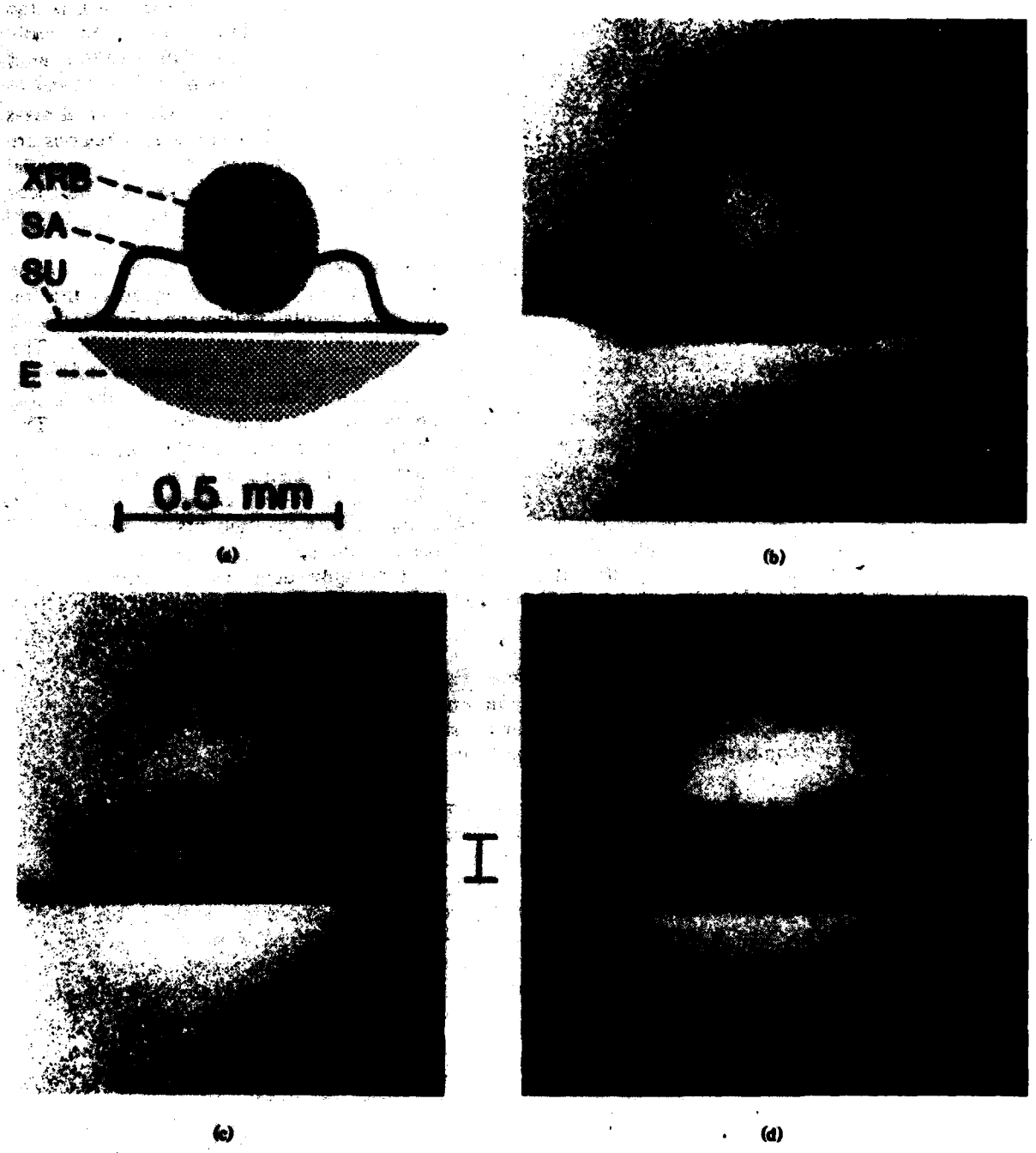

Fig. 2 – (a) Schematic of x radiographs, laser incident from below, including: E self-emission from blowoff of driven foil, SU shadow of unaccelerated margin of foil, XRB x-ray backlit region, and SA shadow of accelerated foil (only part of which is seen in any one radiograph), and distance scale for (b)-(d). Light regions in left corners of radiographs are from nearby pinholes. (b) X radiograph of an 11.2 μm unperturbed target. (c) X radiograph of bar target with 1.05 thickness ratio. Between (c) and (d) is a 140 μm marker. (d) Bar target with 1.15 initial thickness ratio.

Perturbed targets were accelerated under the same illumination conditions. For these targets, the base thickness was 9.7 μm, i.e., about five ablation depths.[12] The bar thickness was systematically increased to 2.7 μm, but all had $\lambda = 50$ μm. A modulation of 50 μm periodicity is observed in the x radiograph of an accelerated foil with 0.5 μm thick bars (Fig. 2c), for an impressed thickness ratio of 1.05 = ((9.7 + 0.5)/9.7). Darker regions correspond to higher x-ray absorption and higher areal mass density. For an increased thickness ratio of 1.15 the striations of higher and lower density regions are more accentuated (Fig. 2d). The mean target displacement was about 140 μm, with dense material extending rearward as far as 200 μm. Larger displacements (accelerations) off the axis of the focus result from an annular region of increased incident irradiance.

In a radiograph of this annular region at the still greater thickness ratio of 1.3, the tips of the denser structures become pronounced and are seen to extend from the accelerated region of the foil proper, back toward the laser. In Fig. 3, we compare the experimental radiograph (Fig. 3a) with numerical simulation results. Note especially the identifications of the spike and bubble regions. The projection of dense mass protrusions back toward the laser (downward in Fig. 3) is characteristic of spikes in the Rayleigh-Taylor instability. In Fig. 3a, a bridge, at least 3 times thinner than the 80 μm ± 5 μm axial extent of the accelerated unperturbed target, appears to connect neighboring spikes. The spikes extend about 60 μm ± 5 μm to the front (toward laser) of this bridge. Smaller projections of mass are also observed to the rear of each spike. Photometric measurements of x-ray intensities[10] in the images of the spike tips and the intervening bubble regions were made with calibrated photographic emulsion.[13] Self-emission of the foil was negligible. Converting these measurements to average mass thicknesses as in Ref. 10 yields densities at least 0.10 of solid in the spikes, assuming an x-ray path length equal to the bar length. Bubble densities are smaller than spike densities by factors of 2.5-4. Accounting for the presence in the x-ray path of the target material at the rim of the focal spot, would increase this factor. The overall axial extent, from tip to rear of the target shadow, is about 105 μm, which is greater than the unperturbed target (80 μm ± 5 μm). These modulations in mass density, and the thinness of the bridge region, indicate that mass redistribution has taken place leaving bubble volumes deficient in mass. The projected radiographic image of the spike tips also appears to exhibit advanced lateral broadening, indicative of the nonlinear stage of the RT instability.[14,15] These highly developed features are compared below with numerical simulation.

The evolution of a perturbed target under conditions similar to those of the experiment was modeled using the FAST2D[3,14] laser-shell simulation code. For the numerical run shown in Fig. 3c, the initial target mass was structured the same as the experimental target of Fig. 3a, while the incident laser intensity was 8×10^{12} W/cm^2 in a $\tau_{laser} = 5$ ns FWHM pulse. The average final target velocity was 3.8×10^6 cm/s and the total distance pushed (measured in the bridge connecting the spikes at $\tau_{delay} = 5$ ns) was 180 μm. Rear surface temperatures were 4-6 eV at τ_{delay}. The most unstable mode, $\lambda = 50\ \mu m = 2\pi/k$, follows an initial phase of amplitude decay while the flow patterns evolve into an eigenmode, then grows exponentially by mass redistribution until $kA \approx 1$, after which the amplitude A of the perturbation grows at the slower free-fall rate,[14] $\Delta A = 1/2 g(\Delta t)^2$, with $g = 1.56 \mu m/ns^2$.

The exponential growth rate was measured numerically to be 7×10^8 s^{-1}, which is about 1.5 times smaller than the linear classical value, in good agreement with the linear growth rates of long wavelength sinusoidal perturbations for constant laser intensity.[14] There were 3 e-foldings of exponential growth above the minimum amplitude. The spike-bubble amplitude (on the 30% density contour) at τ_{delay} is 65 μm (Fig. 3c), which compares favorably with experimental observation (60 μm $\pm 5 \mu$m).

An experimental growth factor of 22 = (60 μm/2.7 μm), over a growth time of no more than $\tau_{delay} + \tau_{laser}$, implies an exponential growth rate greater than $\gamma_{min} = ln(22) + 10$ ns $= 3 \times 10^8\ s^{-1}$. Accounting for initial or free-fall phases of evolution would give larger growth rates. Final amplitude may be compared to a simple model in which exponential growth proceeds at the linear classical rate, and in which the initial phase, the free-fall rate, and the amplitude of transition to free-fall, are as simulated numerically: the calculated final amplitude is greater than that observed by a factor of 1.5.

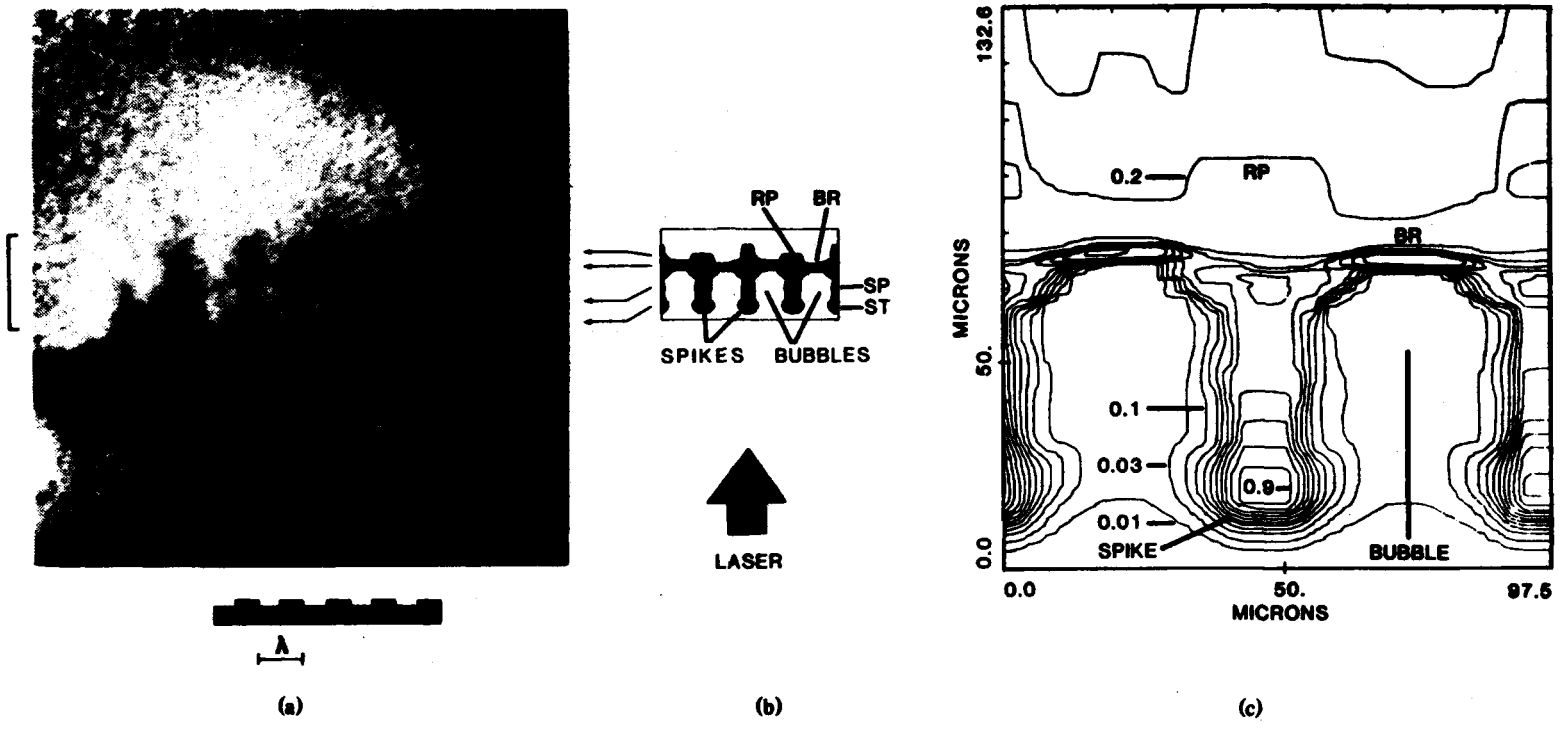

Fig. 3 — Comparison of results for thickness ratio of 1.3 and $\lambda = 50\ \mu m$. Laser incident from below, target acceleration upward, direction of spike growth downward. (a) Experimental x radiograph of bar target. Initial cross-section and scale ($\lambda = 50\ \mu m$, thickness exaggerated) is diagrammed below image. Within the backlit region (upper 2/3 of image), dense target material (including spikes, rear projections, and bridge) appears dark, low density regions (bubbles, area to rear of accelerated target) appear bright. Accelerated target is to right of bracket. (b) Numerical simulation of accelerated target. The 0.2 ρ_{max} contour is demagnified from (c) down to the scale of (a), and repeated to show multiple spikes. Lateral scale of (b) matches (a). Axial positions of corresponding features are conveyed by horizontal arrows extending from (b) to (a). Features of major importance are identified as: spikes, bubbles, ST spike tip, SP spike, BR bridge, RP rear projection. (c) Isodensity contours from FAST2D simulation at τ_{delay}, for conditions given in text. Contours are in 0.10 increments of the maximum ($\rho_{max} = 0.661\ g/cm^3$), with additional contours at 0.03 and 0.01 of ρ_{max}. Bubbles are the large, mass deficient volumes (between the 0.01 and 0.03 contours). Development of spike, bubble, and rear projections, as well as broadening of the spike tips, are evident in these experimental and numerical results.

The nonlinear Kelvin-Helmholtz-like spike-tip broadening[14,15] is clearly evident in Fig. 3c. The vorticity generated by the non-collinear nature of the density and pressure profiles collects behind the heads of the spikes causing the spike tips to widen. This effect becomes appreciable when the amplitude of the perturbation is about half the wavelength of the perturbation.[14] The 20% density contour at the rear of the target, Figs. 3b and 3c, delineates rearside mass projections similar to those found experimentally. These projections in the simulation are due to the collision of mass flowing from adjacent bubble regions into an intermediate spike, resulting not only in spike growth but also in a rearward jetting.[4]

Several mechanisms other than RT were considered: differences in acceleration for thicker and thinner portions of bar targets; preferential thermal broadening of the spike tips; and various geometric mechanisms such as viewing parallax, etc. From the combination of the observed structures and simulation results on temperature contours, the most likely explanation for the structures in the radiographs remains hydrodynamic instability.

In summary, several basic features of the advanced development of the RT hydrodynamic instability have been identified in the numerical results and compared with experimental observations. The observations are consistent with mass redistribution into a high density spike and a mass-deficient bubble, with broadening of the spike tips. Moreover, rearside projections were observed experimentally and interpreted with the numerical simulation results. Mass redistribution processes such as those observed could significantly affect inertial fusion pellet performance. Extensive further experimental work is needed to relate these hydrodynamic phenomena to laser fusion reactor scenarios.

The authors acknowledge helpful discussions with B.H. Ripin, S.E. Bodner, D.B. Brown, J.H. Gardner, J. Grun, and D.J. Nagel. We are further appreciative of the expert technical efforts of J. Bass, D. Cheville, W. Griffith, K.R. Hudson, K. Kearney, W. Naffey, D. Newman, N. Nocerino, M. Rebbert, and E. Turbyfill. This research was supported by the U.S. Department of Energy.

REFERENCES

1. Lord Rayleigh, *Theory of Sound* (Dover, New York, 1945), 2nd ed., Vol. 2; G.I. Taylor, Proc. Roy. Soc. (London), Ser. A 201, 192 (1950).

2. H. Helmholtz, Philos. Mag., Ser. 4, 36, 337 (1868); Lord Kelvin, *Hydrodynamics and General Dynamics* (Cambridge Univ. Press, Cambridge, 1910), pp. 69ff.

3. M.H. Emery, J.H. Gardner, and J.P. Boris, Phys. Rev. Lett. 48, 677 (1982).

4. E. Ott, Phys. Rev. Lett. 29, 1429 (1972); C.P. Verdon, R.L. McCrory, R.L. Morse, G.R. Baker, D.I. Meiron, and S.A. Orszag, Phys. Fluids 25, 1653 (1982).

5. J.N. Shiau, E.B. Goldman, and C.I. Weng, Phys. Rev. Lett. 32, 352 (1974); J. D. Lindl and W. C. Mead, Phys. Rev. Lett. 34, 1273 (1973); G. Fraley, W. P. Gula, D. B. Henderson, R. L. McCory, R. C. Malone, R. J. Mason, R. L. Morse, IAEA-CN-33 F-5-5, Int'l. Atomic Energy Agency, Vienna, 1974.

6. A. Raven, H. Azechi, T. Yamanaka, and C. Yamanaka, Phys. Rev. Lett. 47, 1049 (1981); J.D. Kilkenny, J.D. Hares, C.S. Lewis, and P.T. Rumsby, J. Phys. D 13, L123-5 (1980).

7. B.H. Ripin, S.P. Obenschain, J. Grun, M.J. Herbst, E.A. McLean, J.A. Stamper, R.R. Whitlock, J.M. McMahon, and S.E. Bodner, Bull. Amer. Phys. Soc. 25, 946 (1980); B.H. Ripin, S.E.

Bodner, P.G. Burkhalter, H. Griem, J. Grun, H. Heilfeld, M.J. Herbst, R.H. Lehmberg, C.K. Manka, E.A. McLean, S.P. Obenschain, J.A. Stamper, R.R. Whitlock and F.C. Young, *Plasma Physics and Controlled Thermonuclear Fusion Research 1982*, (IAEA, Vienna, 1983), Vol. I, 139.

8. A.J. Cole, J.D. Kilkenny, P.T. Rumsby, R.G. Evans, C.J. Hooker, and M.H. Key, Nature **299**, 329 (1982).

9. J. Grun, M.H. Emery, M.J. Herbst, E.A. McLean, S.P. Obenschain, B.H. Ripin, J.A. Stamper, and R.R. Whitlock, "Experimental Methods for Studying the Rayleigh-Taylor Instability of Ablatively Accelerated Targets," NRL Memorandum Report 4896, June 17,1983.

10. R.R. Whitlock, S.P. Obenschain, and J. Grun, Appl. Phys. Lett. **41**, 429 (1982).

11. E.A. McLean, S.H. Gold, J.A. Stamper, R.R. Whitlock, H.R. Griem, S.P. Obenschain, B.H. Ripin, S.E. Bodner, M.J. Herbst, S.J. Gitomer, and M.K. Matzen, Phys. Rev. Lett. **45**, 1246 (1980).

12. J. Grun, R. Decoste, B.H. Ripin, and J. Gardner, Appl. Phys. Lett. **39**, 545 (1981).

13. R.F. Benjamin, P.B. Lyons, and R.H. Day, Appl. Opt. **16**, 393 (1977); D. B. Brown, private communication.

14. M.H. Emery, J.H. Gardner, and J.P. Boris, Appl. Phys. Lett . **41**, 808 (1982), and erratum to be published.

15. B. J. Daly, Phys. Fluids **10**, 297 (1967).

END

FILMED

5-84

DTIC